Experimental Observation of Topological Edge States at the Surface Step Edge of the Topological Insulator $ZrTe_5$

Xiang-Bing Li,[1] Wen-Kai Huang,[1] Yang-Yang Lv,[2] Kai-Wen Zhang,[1] Chao-Long Yang,[1] Bin-Bin Zhang,[2] Y. B. Chen,[1,*] Shu-Hua Yao,[2] Jian Zhou,[2] Ming-Hui Lu,[2] Li Sheng,[1,3] Shao-Chun Li,[1,3,†] Jin-Feng Jia,[3,4] Qi-Kun Xue,[5] Yan-Feng Chen,[2,3] and Ding-Yu Xing[1,3]

[1]*National Laboratory of Solid State Microstructures, School of Physics, Nanjing University, Nanjing, Jiangsu 210093, China*

[2]*National Laboratory of Solid State Microstructures, Department of Materials Science and Engineering, Nanjing University, Nanjing, Jiangsu 210093, China*

[3]*Collaborative Innovation Center of Advanced Microstructures, Nanjing University, Nanjing 210093, China*

[4]*Key Laboratory of Artificial Structures and Quantum Control (Ministry of Education), Department of Physics and Astronomy, Shanghai Jiao Tong University, Shanghai 200240, China*

[5]*State Key Laboratory of Low-Dimensional Quantum Physics, Department of Physics, Tsinghua University, Beijing 100084, China*

(Received 14 January 2016; published 28 April 2016)

We report an atomic-scale characterization of $ZrTe_5$ by using scanning tunneling microscopy. We observe a bulk band gap of ~80 meV with topological edge states at the step edge and, thus, demonstrate that $ZrTe_5$ is a two-dimensional topological insulator. We also find that an applied magnetic field induces an energetic splitting of the topological edge states, which can be attributed to a strong link between the topological edge states and bulk topology. The relatively large band gap makes $ZrTe_5$ a potential candidate for future fundamental studies and device applications.

DOI: 10.1103/PhysRevLett.116.176803

A two-dimensional topological insulator (2D TI) is a new type of quantum matter and hosts the quantum spin Hall effect (QSHE) [1,2]. It features an insulating bulk band gap and time-reversal-invariant topological edge states (TESs) protected against localization and backscattering. Since the discovery of the QSHE in the inverted HgTe/CdTe quantum wells [3,4], progress has been made in the predictions and characterizations of 2D TI materials [5–21]. Most of the currently confirmed 2D TIs are of limited practical use, due to either small bulk band gaps or difficulty in achieving thin sheets down to a single layer. Searching for a 2D TI material with practically ideal properties is still of great importance, which, however, is rather challenging. Furthermore, the response of TESs to an applied magnetic field has not been fully understood. Theoretical models have been established to address the spatial distribution of TESs under magnetic fields [22,23], but the energetic evolution has never been studied. Tuning the external magnetic fields or gating voltages, the transition from a 2D TI to a normal insulator or a quantum Hall state could be realized [4,21].

Recently, Weng *et al.* [24] predicted that single layer $ZrTe_5$ is a 2D TI with a large band gap, and the 3D crystal of $ZrTe_5$ is located near the phase boundary between weak and strong topological insulators sensitive to lattice parameters. In contrast, several experimental studies suggested that $ZrTe_5$ might be a Dirac semimetal [25–27]. Therefore, a direct characterization is rather important to clarify the bulk band topology of $ZrTe_5$. In fact, studies of $ZrTe_5$ can be tracked back two decades due to its anomalous magnetoresistance and low-temperature thermoelectric power [28–30].

In this study, we use scanning tunneling microscopy (STM) to characterize the surface of cleaved single crystal $ZrTe_5$. We observe not only a gapped bulk band structure at the surface terrace of the *a-c* plane but also TESs located at the step edge. It then follows that the $ZrTe_5$ surface is a 2D TI, suggesting that the $ZrTe_5$ crystal is a weak 3D TI, in good agreement with the theoretical prediction [24]. In the presence of magnetic field, the edge states undergo a large energy splitting, which could be explained by time-reversal-symmetry-broken edge states closely linked to the bulk band topology [22,23,31].

Single crystal $ZrTe_5$ was grown by the chemical vapor transport method with iodine (I_2) as the transport agent. Polycrystalline $ZrTe_5$ was first synthesized by a solid-state reaction (at about 500 °C for seven days) in a fused silica tube sealed under vacuum (~4×10^{-6} mbar). A ratio of 1:5 for the high purity Zr (99.999%) and Te powder (99.999%) was adopted. The mixture of prepared $ZrTe_5$ polycrystalline and I_2 (~5 mg/L) powder were loaded into a sealed evacuated quartz tube and then put into a two-zone furnace. After growing in a temperature profile of 520 °C–450 °C for over ten days, the single crystal was successfully grown, with a typical size of ~$35 \times 1 \times 0.5$ mm^3.

All STM characterizations were carried out in ultrahigh vacuum (UHV) with a Unisoku LT-STM at ~4 K. The base pressure was 5×10^{-11} mbar. The $ZrTe_5$ single crystal was cleaved *in situ* in UHV and quickly cooled down to 4 K prior to the STM and STS measurements. The constant

current mode was adopted. dI/dV spectra were taken using a lock-in amplifier. A modulation of 5 mV at 1000 Hz was applied. A mechanically polished PtIr tip was used.

The $ZrTe_5$ crystal has an orthorhombic layered structure [32] and contains 2D sheets of $ZrTe_5$ in the a-c plane, which stack along the b axis via interlayer van der Waals interactions, as shown in Fig. 1(a). Each 2D sheet consists of alternating prismatic $ZrTe_3$ chains along the a axis that are linked by parallel zigzag Te chains. The prism of $ZrTe_3$ is formed by a dimer of Te and an apical Te atom surrounding a Zr atom.

$ZrTe_5$ is easily cleavable along the a-c plane, while it also exhibits a quasi-1D preference along the a axis. Figures 1(b) and 1(c) show the topography of such a cleaved $ZrTe_5$ surface, in which Te dimer and Te apical atoms can be well identified. The zigzag chain of Te atoms is right intercalated in between. Note, no charge density wave phase is observed at either 4 or 80 K. The steps are dominantly along the a axis due to the quasi-1D preference, and they are superstraight in mesoscopic scale (approximately a few μm; see Ref. [33]Fig. S1). Such long and straight surface steps make the contact to other quantum material, such as superconductor or ferromagnetic metal, easily controllable. The measured height of a single step is ~0.8 nm. The present STM results are in good agreement with the crystal structure of $ZrTe_5$ [24]. The steps along the

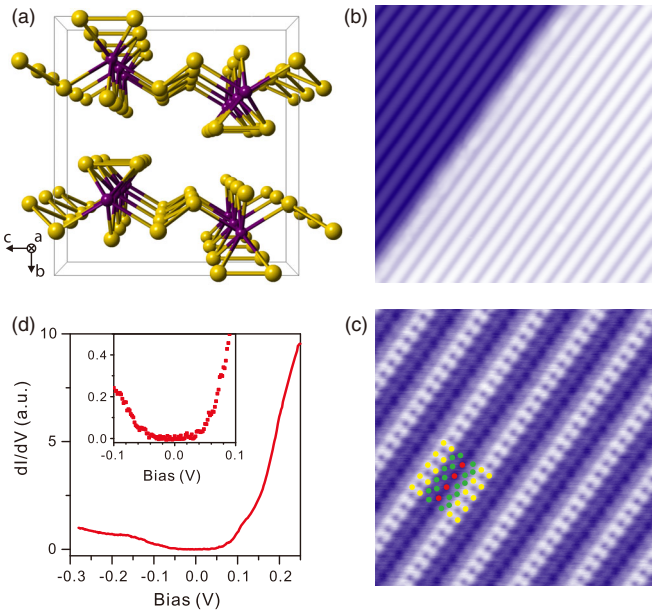

FIG. 1. (a) Crystal structure of $ZrTe_5$. (b) STM image of 25×25 nm^2 obtained at 4 K (bias voltage $U = +1.0$ V, tunneling current $I_t = 100$ pA). The height of the monolayer step is ~0.8 nm. (c) Atomic-resolution image of the $ZrTe_5$ surface (8×8 nm^2, $U = +350$ mV, $I_t = 130$ pA). The yellow balls mark the Te dimers, the red apical Te atoms, and the green zigzag Te atoms. (d) Differential conductance (dI/dV spectra, $U = +250$ mV, $I_t = 200$ pA, Vosc $= 5$ mV) taken over the terrace and far away from the step edge.

c axis are seldom observed, but they are not straight at all (see Ref. [33] Fig. S2).

The local density of states (LDOS, from spectroscopic measurement) obtained at the surface terrace is plotted in Fig. 1(d) and Ref. [33] Fig. S3. Its high homogeneity indicates the high quality of the $ZrTe_5$ single crystal. An energy gap as large as ~80 meV is identified, with the top of the valence band and the bottom of the conductance band located at ~ -35 and $\sim +45$ meV, respectively. This result will be further proven below by the quasiparticle interference analysis at the step edges. The Fermi level is located inside the band gap, but slightly towards the valence band, indicating that the surface terrace is a nearly intrinsic semiconductor. The spectroscopic feature at the $ZrTe_5$ terrace agrees well with the density-functional theory calculation for single layer $ZrTe_5$ [24]. Furthermore, no observable residue states were detected in the band gap region, supporting the model of weak TI rather than strong TI. If it were a strong TI, the residual intensity due to topological surface states would be detectable within the energy gap [24].

To ascertain the electronic structure at the step edge, the LDOS along a line perpendicular to the step edge is plotted in Fig. 2(a). Clearly, the quasiparticle interference due to confinement by the step is observed in the valence and conductance band regions, indicating a 2D-like bulk band structure. In Fig. 2(b), the corresponding 1D fast Fourier transform shows the scattering interference dispersion. The dispersion below the Fermi energy resembles the recent ARUPS results [25]. An energy gap can be also identified between the dispersions for the valence band and conductance band. When approaching the step edge, a couple of new discontinuous peaks appear in the gap region (see, also, the in-gap feature in the fast Fourier transform). In contrast to the spectra at the terrace, the intensity is pronouncedly enhanced near the step edge and spans the whole gap region, indicating the existence of TESs [1,2]. The penetration depth, as measured in the profile perpendicular to the step edge in Fig. 2(c), is ~7.7 and ~6.5 nm for energy near and away from the Fermi level, respectively. This subtle difference can be understood by the argument that the wave function of the edge state penetrates further into the terrace as its energy is closer to the valence or conductance band. The STS measurements at the step along the c axis are analyzed in the Supplemental Material [33] Fig. S4.

Figure 2(d) shows two STM spectra obtained in the surface terrace region [black triangle in Fig. 2(a)] and at the step edge [red triangle in Fig. 2(a)], respectively. The broad bumps located in the valence and conductance band regions arise from the interference at the step edge. The peaks in the gap region are asymmetric, and the 1D character can be further confirmed by fitting the peaks with a 1D density of states exhibiting an inverse-square-root singularity. This characteristic of the edge states recalls the theoretical

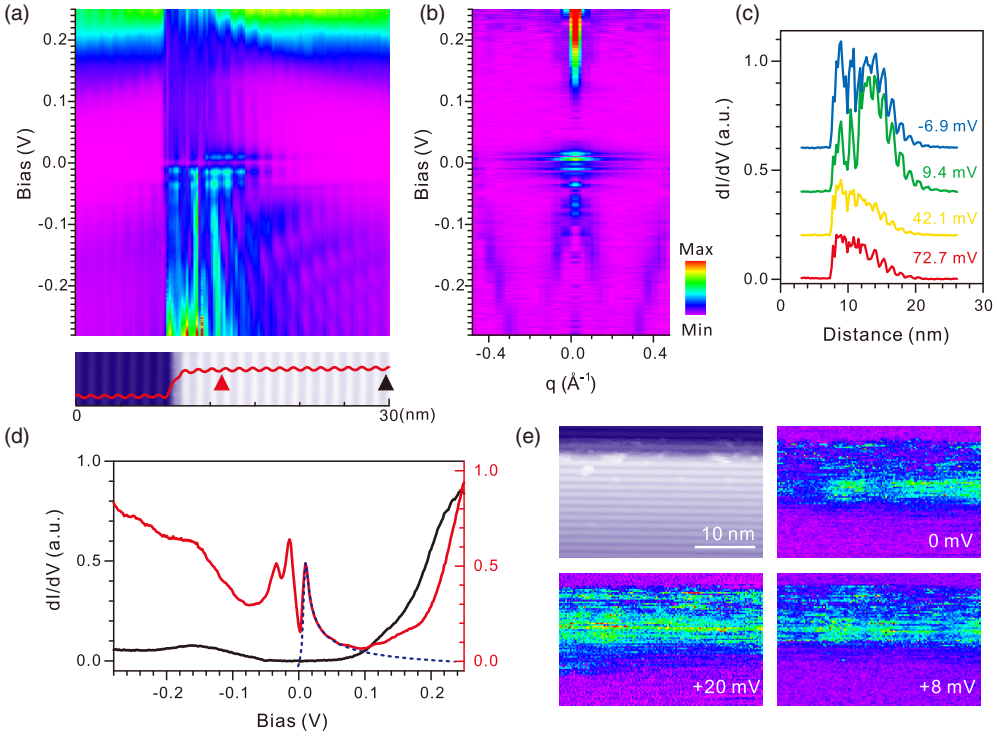

FIG. 2. (a) Differential conductance (dI/dV spectra, $U = +250$ mV, $I_t = 200$ pA, $V_{osc} = 5$ mV) taken across the step. The corresponding step topography is shown below, and the red line profile illustrates the step geometry (30 nm in length). (b) 1D fast Fourier transform of (a) showing the quasiparticle interference. (c) Line cuts at various energies extracted from (a) showing the variation of penetration depth over energy. (d) Two spectra extracted from (a) at the positions marked by black and red triangles. The dotted blue line is the fitting results with a 1D density of states exhibiting the inverse-square-root singularity. The broadening used is ~3 meV. (e) STM topography (34×23 nm^2, $U = +1.05$ V, $I_t = 100$ pA) of another step and the corresponding dI/dV mapping taken at various bias voltages.

calculations for two different types of cuttings of an isolated $ZrTe_5$ single layer [24]. According to the calculated results, the observation of inverse-square-root singularities is expected for the step edge terminated by the zigzag chain rather than by the prismatic chain [24]. Our spectra are more consistent with the zigzag chain terminated steps. Because of the tip curvature effect, it is difficult to identify the exact atomic geometry at the step edge.

The 1D character of the edge states can be further revealed by the spatially resolved spectroscopic mapping along another step. The edge states stay exactly along the step edge, as shown in Fig. 2(e). Since the penetration depth of the edge states is relatively large, the edge channels can circumvent a large-sized perturbation of a few nm, as shown in Fig. 2(e) and Ref. [33] Fig. S5, which is just comparable to the spatial resolution limits for microfabrication techniques. Moreover, the edge states can be observed at all kinds of steps (see Ref. [33] Fig. S5), unlike in the Bi bilayer where the edge states are sensitively coupled to the step geometry [19]. Therefore, the edge states can, in principle, form looped electron channels along the periphery of a $ZrTe_5$ sheet, which can be easily made by microfabrication technology and are rather robust against external perturbations.

An applied magnetic field normal to the surface will break the time-reversal symmetry and drive a complicated evolution of the edge state, as shown in Fig. 3(a) (see, also, Ref. [33] Fig. S6). Three characteristic peaks marked as A, B, and C are tracked for increased magnetic fields. Each peak at energy E is split into two branches with energy difference ΔE, with the corresponding energies shifting up and down, respectively. The intensity for the higher-energy branch is lower than that for the lower-energy one, under relatively high fields. We rule out the possibility of observed bulk Landau quantization based on the following arguments. First, the peak splitting emerges mainly at the step edge, not observable away from the step edge [see Fig. 3(c)]. Second, the splitting is prominent in the gap region where there is no bulk band state. Finally, the evolutions of E [Fig. 3(b) and Ref. [33] Fig. S7] and ΔE [Fig. 3(d) and Ref. [33] Fig. S7] with applied field show neither linear nor parabolic dependence. If the evolutions are the bulk effect, both E vs B and ΔE vs B will exhibit either a linear or parabolic behavior, respectively, corresponding to the bulk Dirac or normal electrons. As a result, the STS spectra in Figs. 3(b) and 3(d) and Ref. [33] Fig. S7 do not come from the bulk band structure but from the TESs. For edge state A_1, the above argument seems

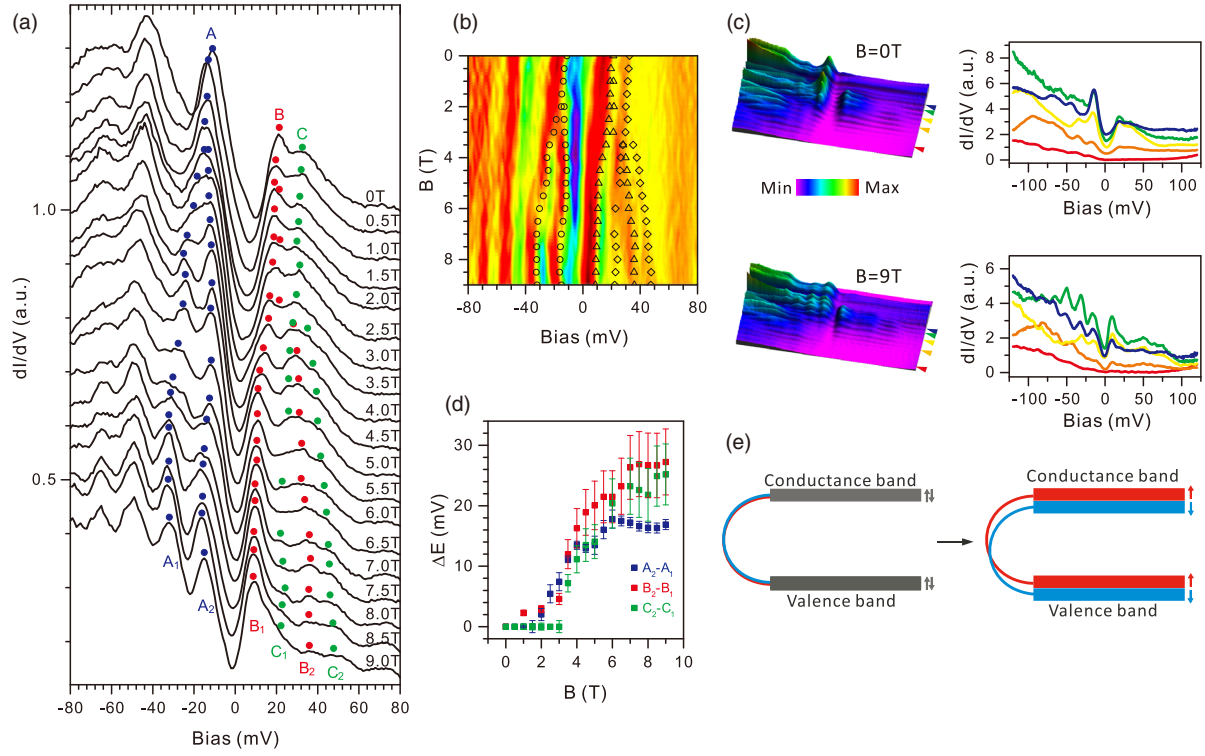

FIG. 3. (a) Differential conductance (dI/dV spectra) obtained at a certain position upon magnetic field, varying from 0 to 9 T, with an increment of 0.5 T. The three peaks in the band gap region are marked as A, B, and C and traced via colored dots, where A splits into A_1, A_2, the same for B and C. (b) The same spectra after differentiation is plotted in false colored mode. The peaks A, B, and C are marked by open circles, triangles, and diamonds. (c) dI/dV spectra ($U = +250$ mV, $I_t = 200$ pA, $V\text{osc} = 5$ mV) taken across the step edge under the magnetic field of 0 (up) and 9 T (down), respectively. Five spectra are extracted and plotted in the right. The corresponding positions for taking the spectra are marked with colored triangles in the left. (d) Energy gap defined as $\Delta E = E_2 - E_1$, vs B. (e) Sketch illustrating the close link between the topological edge states splitting and the magnetic-field-induced bulk quantization. Left and right are sketches without and with an applied magnetic field, respectively.

somewhat lacking of convincing evidence, since its energy is close to the top of the valence band, and there may be a coupling between edge state A_1 and the bulk state. However, states B and C are right inside the band gap and well isolated from the bulk. It was theoretically suggested that an applied magnetic field may open a tiny gap of the edge states at the Dirac point. However, such a tiny gap cannot be distinguished in the present experiment due to the complication of the STS spectra.

Owing to the time-reversal symmetry, the two helical edge states have the symmetric dispersion for opposite momentums, k and $-k$, and the identical spatial distribution. Thus, the two edge states are not distinguishable by STM in the absence of a magnetic field. When the time-reversal symmetry is broken by an external magnetic field, it was theoretically suggested that the two helical edge states persist but are delocalized from the step edge. The favored edge state is pushed further toward the step edge and the unfavored one gradually merges into the bulk [22,23,31]. This scenario can qualitatively explain the decrease in intensity for the higher-energy branch of two splitting peaks. Regardless of the nonlinear dependence of ΔE on B [see Fig. 3(d)], a fitting with $\Delta E = \bar{g}\mu_B B$ roughly gives an effective g factor of 40–60, suggesting that the splitting arises from not only the Zeeman effect but also the orbital effect due to vector potential [27,34]. Furthermore, the effective g factor is comparable to the value for bulk Landau quantization obtained in a magnetoinfrared spectroscopy study [27]. Therefore, we conclude that the edge state evolution is highly correlated with the bulk band topology. The schematic shown in Fig. 3(e) illustrates the magnetic-field-induced Landau quantization and Zeeman splitting of the bulk band, which results in an effective splitting of the corresponding edge states. This simple model can qualitatively explain the experiment, but, in fact, the evolution will be much more complicated if the bulk band and edge state symmetries are taken into account, as seen from the unusual dependence of ΔE on B. Further theoretical and experimental investigations, especially under higher magnetic field, are required to fully understand the physical mechanism.

In summary, we have shown that the $ZrTe_5$ surface is a 2D TI with bulk band gap and topological edge states located at the surface step edge. This suggests that the

$ZrTe_5$ is a weak 3D TI rather than a Dirac semimetal. This material is easily cleavable, the band gap of the surface terrace is relatively large, and the surface step edges obtained are ultralong and ultrastraight. The topological edge states are found rather robust against nonmagnetic perturbations. In addition, we have also studied the evolution of the edge states in the presence of an increased magnetic field, which can be understood by a theoretical model of the time-reversal-symmetry-broken topological edge states.

This work was supported by the State Key Program for Basic Research of China (Grants No. 2014CB921103, No. 2015CB921203, and No. 2013CB922103), National Natural Science Foundation of China (Grants No. 11374140, No. 11374149, No. 51032003, No. 50632030, No. 10974083, No. 51002074, No. 10904092, and No. 51472112), and the New Century Excellent Talents in University (Grant No. NCET-09-0451).

X.-B. L., W.-K. H., and Y.-Y. L contributed equally to this work.

Note added.—Recently, we found that similar conclusions were reached independently in Ref. [35].

*Corresponding Author.
ybchen@nju.du.cn
†Corresponding Author.
scli@nju.edu.cn

[1] M. Z. Hasan and C. L. Kane, Rev. Mod. Phys. **82**, 3045 (2010).
[2] X.-L. Qi and S.-C. Zhang, Rev. Mod. Phys. **83**, 1057 (2011).
[3] B. A. Bernevig, T. L. Hughes, and S.-C. Zhang, Science **314**, 1757 (2006).
[4] M. König, S. Wiedmann, C. Brüne, A. Roth, H. Buhmann, L. W. Molenkamp, X.-L. Qi, and S.-C. Zhang, Science **318**, 766 (2007).
[5] X. Qian, J. Liu, L. Fu, and J. Li, Science **346**, 1344 (2014).
[6] S. M. Nie, Z. D. Song, H. M. Weng, and Z. Fang, Phys. Rev. B **91**, 235434 (2015).
[7] M. A. Cazalilla, H. Ochoa, and F. Guinea, Phys. Rev. Lett. **113**, 077201 (2014).
[8] R. Roy, Phys. Rev. B **79**, 195322 (2009).
[9] C. C. Liu, W. X. Feng, and Y. G. Yao, Phys. Rev. Lett. **107**, 076802 (2011).
[10] Y. Xu, B. H. Yan, H. J. Zhang, J. Wang, G. Xu, P. Z. Tang, W. H. Duan, and S. C. Zhang, Phys. Rev. Lett. **111**, 136804 (2013).
[11] C. L. Kane and E. J. Mele, Phys. Rev. Lett. **95**, 226801 (2005).
[12] A. Shitade, H. Katsura, J. Kunes, X. L. Qi, S. C. Zhang, and N. Nagaosa, Phys. Rev. Lett. **102**, 256403 (2009).
[13] C. Liu, T. L. Hughes, X.-L. Qi, K. Wang, and S.-C. Zhang, Phys. Rev. Lett. **100**, 236601 (2008).
[14] S. Murakami, Phys. Rev. Lett. **97**, 236805 (2006).
[15] B. Rasche, A. Isaeva, M. Ruck, S. Borisenko, V. Zabolotnyy, B. Buchner, K. Koepernik, C. Ortix, M. Richter, and J. van den Brink, Nat. Mater. **12**, 422 (2013).
[16] A. Roth, C. Brune, H. Buhmann, L. W. Molenkamp, J. Maciejko, X. L. Qi, and S. C. Zhang, Science **325**, 294 (2009).
[17] F. F. Zhu, W. J. Chen, Y. Xu, C. L. Gao, D. D. Guan, C. H. Liu, D. Qian, S. C. Zhang, and J. F. Jia, Nat. Mater. **14**, 1020 (2015).
[18] C. Pauly, B. Rasche, K. Koepernik, M. Liebmann, M. Pratzer, M. Richter, J. Kellner, M. Eschbach, B. Kaufmann, L. Plucinski, C. M. Schneider, M. Ruck, J. van den Brink, and M. Morgenstern, Nat. Phys. **11**, 338 (2015).
[19] I. K. Drozdov, A. Alexandradinata, S. Jeon, S. Nadj-Perge, H. Ji, R. J. Cava, B. Andrei Bernevig, and A. Yazdani, Nat. Phys. **10**, 664 (2014).
[20] F. Yang, L. Miao, Z. F. Wang, M. Y. Yao, F. Zhu, Y. R. Song, M. X. Wang, J. P. Xu, A. V. Fedorov, Z. Sun, G. B. Zhang, C. Liu, F. Liu, D. Qian, C. L. Gao, and J. F. Jia, Phys. Rev. Lett. **109**, 016801 (2012).
[21] I. Knez, R.-R. Du, and G. Sullivan, Phys. Rev. Lett. **107**, 136603 (2011).
[22] H. Li, L. Sheng, R. Shen, L. B. Shao, B. Wang, D. N. Sheng, and D. Y. Xing, Phys. Rev. Lett. **110**, 266802 (2013).
[23] G. Tkachov and E. M. Hankiewicz, Phys. Rev. Lett. **104**, 166803 (2010).
[24] H. Weng, X. Dai, and Z. Fang, Phys. Rev. X **4**, 011002 (2014).
[25] Q. Li, D. E. Kharzeev, C. Zhang, Y. Huang, I. Pletikosic, A. V. Fedorov, R. D. Zhong, J. A. Schneeloch, G. D. Gu, and T. Valla, arXiv:1412.6543v1.
[26] R. Y. Chen, S. J. Zhang, J. A. Schneeloch, C. Zhang, Q. Li, G. D. Gu, and N. L. Wang, Phys. Rev. B **92**, 075107 (2015).
[27] R. Y. Chen, Z. G. Chen, X. Y. Song, J. A. Schneeloch, G. D. Gu, F. Wang, and N. L. Wang, Phys. Rev. Lett. **115**, 176404 (2015).
[28] T. M. Tritt, N. D. Lowhorn, R. T. Littleton, A. Pope, C. R. Feger, and J. W. Kolis, Phys. Rev. B **60**, 7816 (1999).
[29] R. T. Littleton, T. M. Tritt, J. W. Kolis, and D. R. Ketchum, Phys. Rev. B **60**, 13453 (1999).
[30] T. E. Jones, W. W. Fuller, T. J. Wieting, and F. Levy, Solid State Commun. **42**, 793 (1982).
[31] H. Li, L. Sheng, and D. Y. Xing, Phys. Rev. Lett. **108**, 196806 (2012).
[32] H. Fjellvag and A. Kjekshus, Solid State Commun. **60**, 91 (1986).
[33] See Supplemental Material at http://link.aps.org/supplemental/10.1103/PhysRevLett.116.176803 for supplemental STM and STS data taken on $ZrTe_5$ surface terrace and steps.
[34] S. Jeon, B. B. Zhou, A. Gyenis, B. E. Feldman, I. Kimchi, A. C. Potter, Q. D. Gibson, R. J. Cava, A. Vishwanath, and A. Yazdani, Nat. Mater. **13**, 851 (2014).
[35] R. Wu, J.-Z. Ma, L.-X. Zhao, S.-M. Nie, X. Huang, J.-X. Yin, B.-B. Fu, P. Richard, G.-F. Chen, Z. Fang, X. Dai, H.-M. Weng, T. Qian, H. Ding, and S. H. Pan, arXiv:1601.07056 [Phys. Rev. X (to be published)].